JACS
JOURNAL OF THE AMERICAN CHEMICAL SOCIETY

Article

pubs.acs.org/JACS

Post-Synthesis Incorporation of ^{64}Cu in CuS Nanocrystals to Radiolabel Photothermal Probes: A Feasible Approach for Clinics

Andreas Riedinger,[†,∥,⊥] Tommaso Avellini,[†,⊥] Alberto Curcio,[†,⊥] Mattia Asti,[‡] Yi Xie,[†] Renyong Tu,[†] Sergio Marras,[†] Alice Lorenzoni,[§] Sara Rubagotti,[‡] Michele Iori,[‡] Pier Cesare Capponi,[‡] Annibale Versari,[‡] Liberato Manna,[†] Ettore Seregni,[§] and Teresa Pellegrino*[,†]

[†]Istituto Italiano di Tecnologia, Via Morego 30, 16163, Genova, Italy

[‡]Nuclear Medicine Unit, Oncology and Advanced Technologies Department, Arcispedale Santa Maria Nuova-IRCCS, Viale Risorgimento 80, 42121, Reggio Emilia, Italy

[§]Division of Nuclear Medicine, Istituto Nazionale per lo Studio e la Cura dei Tumori, Via Venezian 1, 20133 Milano, Italy

[∥]Optical Materials Engineering Laboratory, ETH Zurich, 8092 Zurich, Switzerland

Supporting Information

ABSTRACT: We report a simple method for the incorporation of Cu(I) or ^{64}Cu(I) radionuclides in covellite nanocrystals (CuS NCs). After the in situ reduction of Cu(II) or ^{64}Cu(II) ions by ascorbic acid, their incorporation in PEG-coated CuS NCs takes place at room temperature. In all the reaction steps, the stability of the NCs under physiological conditions was ensured. The copper incorporation reaction could also take place on CuS NCs bearing biotin molecules at their surface, with no detrimental effects on the specific binding affinity of the NCs toward streptavidin after incorporation. At low loading of Cu ions, the strong near-infrared (NIR) absorption band of the starting CuS NCs was essentially preserved, which allowed for efficient plasmonic photothermal therapy. The combined presence in the NCs of ^{64}Cu ions, well suitable for positron emission tomography, and of free carriers responsible for the NIR absorption, should enable their theranostic use as radiotracers and as photothermal probes in tumor ablation treatments. Moreover, the simplicity of the preparation scheme, which involves the use of radioactive species only as a last step, makes the protocol easily transferable to the clinical practice.

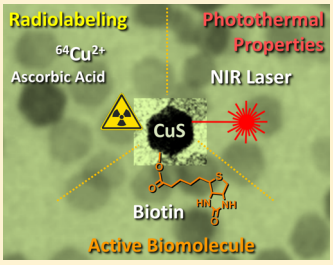

INTRODUCTION

In the medical practice, ^{64}Cu is a valuable radioisotope for both positron emission tomography (PET), as it emits β^+ particles, and for radiotherapy, as it also emits β^- particles.[1−3] Unfortunately, currently available clinical therapies based on ^{64}Cu-radiolabeled peptides or antibodies are limited by the accumulation of the radiopeptides to excretion organs, with unwanted side effects (i.e., nephrotoxicity). To overcome these limitations, various attempts have been made to associate ^{64}Cu radionuclides to nanocrystals (NCs). The most common strategy resides in the use of suitable metal chelators anchored to the surface of the NCs.[4,5] Following this approach, ^{64}Cu ions were associated with magnetic NCs[6−8] and to fluorescent quantum dots.[9,10] One major concern of this strategy is that a large number of metal cations, bound to the surface of the NCs, will inevitably affect the surface properties and will additionally reduce the portion of NC's surface space available for binding targeting molecules or drugs.[11] Since surface properties usually determine the fate of NCs in biological systems, the use of NCs bearing surface anchored cations would then require fine-tuning of the experimental conditions for each specific application. Besides, issues related to stability and/or dissociation of the metal ions from the chelators must be taken into account when exposing such radiolabeled NCs to the saline environment of physiological media.[12,13] As an example, Parak et al. have recently demonstrated that, even if the radiotracer is well bound to the chelator, once the NCs are injected into rats, part of the degradation of the organic surface capping layer (that carries the chelator) causes the dissociation of the radioisotope from the NC.[14]

To circumvent these issues, the direct insertion of ^{64}Cu ions inside the NCs rather than at the NC's surface (as in the chelating methods discussed above) has been proposed. This is done by mixing ^{64}Cu salts with the other precursors needed for the synthesis during the preparation of the NCs. The ^{64}Cu precursors are customarily referred to as the "hot precursors", in order to distinguish them from the nonradioactive Cu precursors, which are termed instead "cold precursors". With this approach, various types of ^{64}Cu doped NCs have been prepared, for example glutathione-coated ^{64}Cu-copper metal NCs,[15] ^{64}Cu−Au alloy NCs,[16] and ^{64}Cu:CuS NCs.[17] Another reported strategy for introducing ^{64}Cu in the NCs is by partial cation exchange. Sun et al. doped hydrophobic CdSe/ZnS NCs of various sizes in a hexane/ethanol mixture at 60 °C with ^{64}Cu(I) by in situ reduction of $^{64}CuCl_2$ with ascorbic acid,[18] followed by partial exchange of the Zn(II) and/or Cd(II) cations of the NCs with ^{64}Cu(I). These radiolabeled-QDs were

Received: July 29, 2015
Published: November 9, 2015

DOI: 10.1021/jacs.5b07973
J. Am. Chem. Soc. 2015, 137, 15145−15151

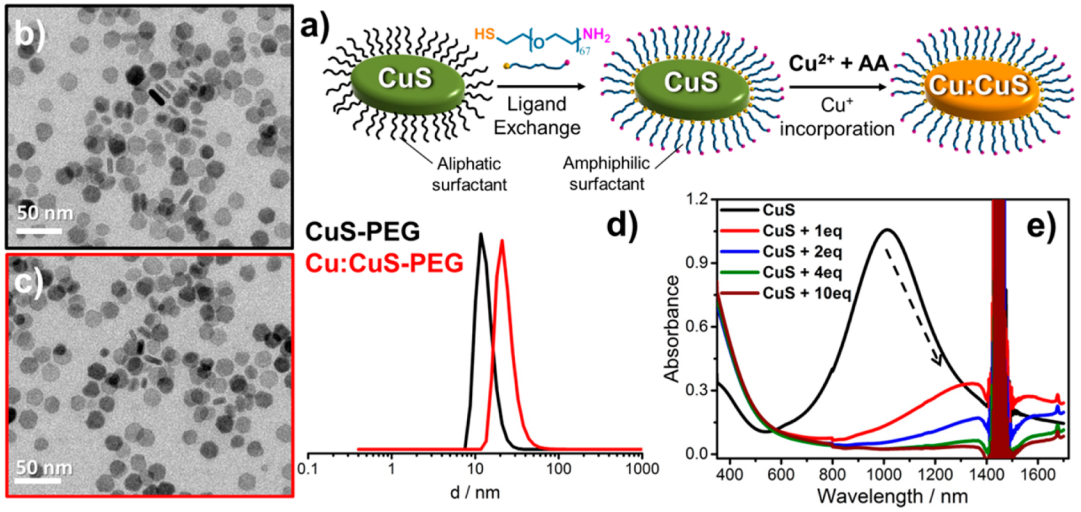

Figure 1. (a) Sketch summarizing the water transfer process by means of ligand exchange on covellite CuS NCs and Cu(I) incorporation starting with Cu(II) and ascorbic acid (AA) as precursors. (b) Representative TEM image of CuS NCs stabilized with SH-PEG-NH_2 (scale bar is 50 nm) and (c) TEM image of CuS NCs after Cu(I) incorporation (scale bar is 50 nm). (d) Hydrodynamic diameter (number mean) of CuS NCs before (black line) and after (red line) the Cu(I) incorporation reaction took place in PBS media. (e) Absorption spectra of CuS NCs after 5 min reaction with different equivalents of $CuCl_2$ salt in the presence of AA.

then transferred in water. The luminescent properties were retained after partial cation exchange and water transfer, and the NCs exhibited efficient Cerenkov resonance energy transfer. Together with positron emission by the ^{64}Cu decay, which allowed PET imaging, these NCs could enable bimodal (photoluminescent and PET) tumor imaging.[18] These NCs were excellent for imaging but lacked therapeutic properties. Instead, the citrate-stabilized ^{64}Cu:CuS NCs prepared by Zhou et al. following an in situ ^{64}Cu incorporation during the NC synthesis[17] offered combined PET imaging and photothermal treatment. This is because CuS is characterized by a strong near-infrared (NIR) absorption band, arising from the presence of free carriers,[19] and therefore, the ^{64}Cu:CuS NCs, after polyethylene glycol (PEG) stabilization, were able to dissipate heat when irradiated with a laser at 808 nm.

The main limitation of all these reported syntheses is that the radioactive material is never introduced at the last step of the preparation pipeline: it is either involved early in the synthesis, or it is introduced after the synthesis, by cation exchange, however, before the water transfer and purification steps. All these procedures require a chemistry laboratory equipped with radio-safety facilities, and this makes the protocols rather difficult to be translated in clinic. Moreover, these reactions often require temperature conditions that are not always suitable for NCs bearing bioactive molecules: reaction temperatures higher than 40 °C would eventually denature proteins or biomolecules attached to the NC's surface. Also, given the relative short half-life of ^{64}Cu (of about 12.7 h), the time needed for performing all the synthetic steps will inevitably reduce the actual radioactive dose that can be delivered by the NCs when they are administered to the patient.[1,20] These limitations call for the development of radiolabeling protocols that are more efficient and easily transferable in clinic overcoming the limitations of the current preparation methods of ^{64}Cu labeled nanocrystals, and that eventually deliver NCs with combined imaging and therapeutic properties.

Our starting point in the present work is based on the evidence that ^{64}Cu:CuS NCs can combine PET imaging and photothermal treatment,[17] and it further builds on the demonstrated capability of CuS (covellite) NCs to incorporate Cu(I) ions, as shown by us[21] in a previous work, although such incorporation was proven so far only in nonaqueous media. Here, we have developed instead a radiolabeling protocol consisting in the in situ reduction of ^{64}Cu(II) ions to ^{64}Cu(I) ions, followed by their incorporation in covellite NCs. All reactions were carried out in an aqueous environment on NCs decorated at their surface either with PEG molecules or with biotin-PEG molecules that provide, at the same time, solubility of the NCs in physiological media and targeting abilities. The incorporation reaction was nearly complete within a few minutes at room temperature and was not hindered by the hydrophilic coatings or by the presence of biotin molecules at the NC's surface. Moreover, the binding efficiency of the biotin functionalities at the NC's surface was not affected by the copper incorporation reaction. Even more important, the ^{64}Cu incorporation reaction represents in our case the very last step of manipulation of the NCs, hence the exposure time of the operators to radioactivity is minimized. Also, in principle, the ^{64}Cu incorporation procedure can be performed just a few minutes before the NCs are administered to the patient. This should ensure high specific activities of the NCs, since waiting times are reduced to a minimum and barely any ^{64}Cu decays during this last period. At low dose of incorporation of the Cu(I) ions in the covellite NCs, the particles preserved most of the their NIR absorbance and consequently their photothermal efficiency upon laser irradiation.[17,22] All together, these results represent a significant progress toward the translation of ^{64}Cu:CuS NCs to clinical routines.

RESULTS AND DISCUSSION

Our group has previously shown that covellite NCs dispersed in a nonaqueous solvent (toluene) could incorporate Cu(I) ions, which were introduced in the reaction medium as a $[Cu(CH_3CN)_4]PF_6$ complex, at room temperature. The stoichiometry in the resulting NCs could be tuned from roughly $Cu_{1.1}S$ all the way to Cu_2S.[21] Inspired by this reaction scheme, and driven by the need to define preparation steps that can be easily translated into clinic, we have developed a copper

DOI: 10.1021/jacs.5b07973
J. Am. Chem. Soc. 2015, 137, 15145−15151

incorporation protocol that works on water stabilized NCs. The as-synthesized covellite CuS NCs (see Figure S1 of the Supporting Information, SI) were soluble in solvents like toluene or chloroform, and therefore had to be transferred in water first. This was done by means of a ligand exchange procedure (Figure 1a). In toluene, SH-PEG-NH_2 molecules (3000 g mol^{-1}) were mixed with the as-synthesized CuS NCs (coated by aliphatic surfactants) to a ratio of 42 000 SH-PEG-NH_2 molecules per NC (83 SH-PEG molecule/nm^2), followed by the addition of water. A biphasic mixture was then formed, and, after 1 h of vigorous shaking, the replacement of the aliphatic surfactants with the SH-PEG-coated CuS NCs promoted the extraction of the latter from the toluene phase to the aqueous phase. The excess of free SH-PEG-NH_2 was then removed by means of several cycles of dialysis using centrifugal filters. The mercapto-PEG stabilized CuS NCs retained their shape and their morphology upon water transfer and had a narrow distribution of hydrodynamic diameters (peaked at 19 nm, see black plot of Figure 1d), which indicates the presence of individually coated NCs in water, hence the absence of agglomerates.

A second requirement of a radiolabeling protocol is that only radioisotope salts which are regularly provided by the cyclotron facility can be employed. As ^{64}Cu is provided as an aqueous solution of $^{64}CuCl_2$ in HCl 0.1 N, the incorporation conditions had to be adapted to suit this specific type of solution. Tests were run first using nonradioactive (that is, "cold") $CuCl_2$ in HCl 0.1 N as copper source, so that $^{64}CuCl_2$ would be then used only after the protocol had been optimized. First, the pH of the $CuCl_2$ solution at various concentrations (from 0.7 to 7 mM) had to be adjusted by addition of NaOH (0.1 N) to avoid decomposition of the CuS NCs. Then, CuS NCs (50 nM) were added to the $CuCl_2$ solution. In all cases, no changes to the plasmonic band in NCs spectra were detected after mixing, even after several hours at room temperature (see Figure S5 of the SI). This indicates that Cu(II) ions cannot be incorporated in covellite CuS NCs, a result that is in line with our previously published results,[21] according to which only the presence of Cu(I) ions could trigger the incorporation of copper in the NCs. To efficiently reduce Cu(II) to Cu(I) in situ, we chose vitamin C (ascorbic acid, AA) as a nontoxic and mild reducing agent. As soon as an excess of AA was mixed with the solution (we worked at a ratio of AA to Cu ions equal to 6:1), an immediate change of the solution color from dark green to light brown was observed. Optical spectra of the solutions (Figure 1e), taken 5 min after the addition of AA, evidenced both a significant decrease in intensity and a red shift of the covellite plasmon band from 1060 to 1400 nm and beyond, which were more marked when the amount of $CuCl_2$ added to the CuS NC solution was increased from 1 to 10 equiv (in the case of 1 equiv the concentration of $[Cu_{added}] = [Cu_{NC}]$ while we systematically increase it up to 10-fold). Such spectral changes and their dependence on the amount $CuCl_2$ added (in the presence of a reducing agent) are indicative of incorporation of an increasing fraction of Cu(I) ions and are in line with our previous studies on CuS NCs in the toluene phase (apart from the strong absorption between 1400 and 1500 nm, which is due to water).[21]

The increase in Cu content in the NCs was directly proven by comparing elemental analyses (via inductively coupled plasma atomic emission spectroscopy, ICP-AES) of CuS NCs before and after the reaction carried out at pH 7 (in the latter case, after the NCs had been separated from reaction solution). The analyses indicated an evolution in NC stoichiometry from 1.1 of the initial NCs, to 1.34 (when using 1 equiv of $CuCl_2$) and then to 1.45 (when using 2 equiv of $CuCl_2$). Also, XRD analysis on a sample that went through quantitative incorporation indicated an evolution from a pattern that could be well matched with the covellite phase to a pattern, after Cu incorporation, that contained contributions from higher chalcocite (see Figure S3 of the SI). This is in line with our previous findings for a similar reaction scheme carried out in toluene.[21] For elemental analysis, as well as for any further processing of the NCs, the purification from ascorbic acid and from excess of copper ions was done by filtration of the reaction solution through a size exclusion column (NAP column). The NCs were less retained on the columns and were eluted first, while the free Cu ions were significantly retarded and were released much later, thus allowing recovery of the purified Cu:CuS NCs. As a note, after those steps, a partial reoxidation of the Cu-rich covellite took place, as confirmed by the appearance of a shallow plasmon band (see Figure S7 of the SI).

The incorporation of copper had no appreciable effect on the size and shape of the initial PEG coated NCs (as observed by TEM, Figure 1b and 1c). Instead, a slight increase of the DLS diameter was observed, although no change on the colloidal stability of the Cu:CuS NCs was detected (Figure 1 d).Thermogravimetric analysis (TGA) was also performed in order to assess whether the Cu(I) incorporation reaction leads to the detachment of a measurable fraction of ligands from the NC's surface.

In TGA, the weight loss can be directly correlated to the organic fraction in the NCs (hence to their ligand shell), since the inorganic cores should resist the TGA treatment at moderate temperatures. Therefore, any difference in weight loss between the initial CuS sample and the Cu:CuS sample recorded by TGA can be ascribed to a difference in the density of ligands at the NC's surface between the two samples. TGA analysis indeed evidenced that the ligand shell weighed 12% less in the Cu:CuS sample compared to the initial CuS sample. In terms of the number of PEG ligand molecules per individual NC, the Cu incorporation reaction entailed then a drop of such number from 630 to 460 PEG per NC. Nonetheless, the NCs appeared to withstand this reduction in the number of surface ligands, as their colloidal stability was not compromised. Additional details can be found in the SI (Figure S4).When a large excess of Cu(II) equivalents was used (from 5 equiv and more), even though the starting $CuCl_2$ salt was completely soluble, the Cu(I) ions generated in situ upon addition of AA were only partially soluble in water. In this case, the addition of acetonitrile (ACN) to the reaction medium, acting as complexing agent for Cu(I), was required. In the case of 1 or 2 equiv of initial $CuCl_2$ added to the CuS NCs, such addition was not necessary, since the concentration of Cu(I) ions produced was below the solubility limit of CuCl in water (the solubility product constant of CuCl is 1.72×10^{-7}).[23] Interestingly, by increasing the amount of ACN present in the reaction mixture, a progressive hypsochromic shift (from above 1400 to 1100 nm) of the NIR plasmon band of the resulting NCs suspension was recorded. This trend corroborates an increased stability of the Cu(I) ions in solution and a consequent hindering of the Cu(I) incorporation reaction (Figure S2 of the SI).

We then proceeded to attempt a prototypical labeling experiment using a $^{64}CuCl_2$ solution. Henceforth, we will refer

DOI: 10.1021/jacs.5b07973
J. Am. Chem. Soc. 2015, 137, 15145−15151

to the activity of the ^{64}Cu radioisotope (in MBq or mCi), rather than to the absolute concentration of Cu ions. For safety reasons, we worked with $^{64}CuCl_2$ at around 37 MBq (or 1 mCi) of activity per experiment. Nonetheless, the simplicity of our protocol makes it easily scalable. With proper protection measures, the activity potentially could be increased until a composition equal to ^{64}Cu:CuS (equivalent to Cu_2S) is reached. The reactions were then carried out and the effect of different pH values on the labeling was studied. An activity of 37 MBq corresponds to an overall amount of 0.3 ng of ^{64}Cu. Concentration ratios were set such that, even when only a few ^{64}Cu ions per NC were incorporated, the activity of the resulting ^{64}Cu:CuS NC was still sufficient for PET. At the same time, the NCs still preserved much of their NIR absorbance and exhibited a good heating performance when excited with a NIR laser. In these radiolabeling experiments, the concentration of NCs remained fixed (as in the previous set of experiments employing "cold" $CuCl_2$), while the amount of ^{64}Cu solution added was varied. A dose calibrator was employed to measure the radionuclide activity on the ^{64}Cu:CuS NCs. Measurements were done after purification on a NAP column, on the first collected fraction that contained the NCs, while free-^{64}Cu ions were blocked in the cartridge and were not eluted further.

For convenience, we define here the radiochemical yield (RCY) as the ratio between the starting $^{64}CuCl_2$ activity and the activity associated with the ^{64}Cu:CuS NC after the purification processes. Instead, the radiochemical purity (RCP) is defined as the fraction of the stated isotope present in the stated chemical form. In our experiments, both the RCY and the RCP of the NCs were strongly dependent on the pH at which the ^{64}Cu incorporation reaction was performed. As summarized in Figure 2b, in both reactions carried out at pH 3 and pH 10, RCYs were low and unacceptable for a radiopharmaceutical preparation. Conversely, for incorporations performed at pH 5.5, a RCP over 99% was found, resulting in an overall radiochemical yield of 49%. Based on the specific activity of the precursor (3.7 GBq/μg or 100 mCi/μg), we can estimate that a total amount of 0.01 μg of Cu(II) was involved in the reaction, although the amount of ^{64}Cu should be only around 0.3 ng.

Taking into account a RCY of around 50%, the moles of NC (3.9×10^{-11} moles) and the total moles of copper ions used in a single incorporation reaction (4×10^{-12} moles, considering that ^{64}Cu(II) ions represent just 3% of the total copper content), and also that the highest RCY obtained was 49%, we calculated that, on average, one NC every 16 would be then radiolabeled. In a control experiment performed at pH 5.5 using cold copper at a much higher concentration ($[Cu_{added}] = [Cu_{NC}]$), elemental analysis showed that the Cu/S atom ratio in the Cu:CuS NCs after copper incorporation at pH 5.5 was equal to 1.57. This copper loading efficiency is fully in line with the efficiency obtained by considering RCY for the "hot" reaction. This Cu:S ratio found with the reaction at pH 5.5 was higher than the one found under the same experimental conditions at pH 7 and which delivered instead a Cu/S ratio of 1.35. This suggests that pH 5.5 is the most suitable pH for the ^{64}Cu incorporation. The quality assessment of the radiolabeling was done by using thin layer chromatography (TLC) and agarose gel electrophoresis (AGE) on purified ^{64}Cu:CuS NCs and free ^{64}Cu(II) as reference. On TLC, the retention factor for ^{64}Cu:CuS NCs was equal to 0.1, while for free ^{64}Cu(II) it was equal to 0.8. Less than 1% of free ^{64}Cu could be detected in the final product. Note that, under ambient conditions, any free ^{64}Cu(I) species would rapidly oxidize to ^{64}Cu(II) and thus would show up in TLC with a retention factor of 0.8 (see Figure S6 of the SI). AGE analysis (Figure 2a) evidenced a significant difference in the mobility of free ^{64}Cu(II) and ^{64}Cu:CuS NCs in the agarose gel; hence, the two species were clearly distinguishable. After 10 min at 100 V, the positively charged, free ^{64}Cu(II) ions moved under the electric field toward the negative pole, while the ^{64}Cu:CuS NCs were mainly retained at the deposition point (black dashed line). The stability of the ^{64}Cu:CuS NCs prepared at pH 5.5 was assessed over a period of up to 24 h by incubating the sample at 37 °C with a 0.9% NaCl solution and human blood. Activity distributions were analyzed by TLC at 1 h, 4 and 24 h and compared with the chromatogram obtained from ^{64}Cu:CuS NCs solution before the incubation (t = 0 h) (Figure 2c). At 0 h, the RCP was over 99%, meaning that all the ^{64}Cu species present were colocalized with the NCs on the TLC and no free ^{64}Cu was detected on the TLC slide, while after 24 h the RCP had decreased to 78% in 0.9% NaCl solution and to 60% in human blood, respectively (see also in Figure S6 of the SI for the complete report on the stabilities over time in the two media).

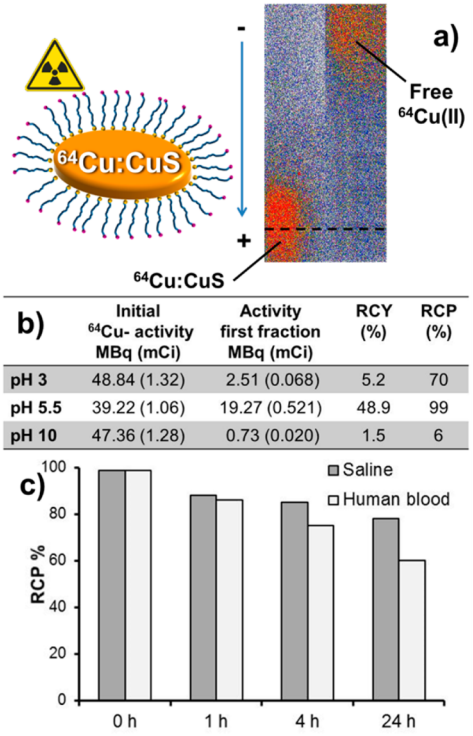

b)

	Initial ^{64}Cu- activity MBq (mCi)	Activity first fraction MBq (mCi)	RCY (%)	RCP (%)
pH 3	48.84 (1.32)	2.51 (0.068)	5.2	70
pH 5.5	39.22 (1.06)	19.27 (0.521)	48.9	99
pH 10	47.36 (1.28)	0.73 (0.020)	1.5	6

Figure 2. (a) Agarose gel electrophoresis analysis (running buffer: borate pH 9 on 2.5% agarose gel with a run of 30 min at 100 V) of free ^{64}Cu(II) and ^{64}Cu:CuS NCs measured in a dose calibrator. (b) Analysis of ^{64}Cu(I) incorporation reactions performed at different pH values. (c) Stability of ^{64}Cu:CuS NCs (prepared at pH 5.5) in 0.9% saline solution and human blood.

To further prove that the incorporation reaction could take place even in CuS NCs having bioactive molecules at their surface, biotin was linked to the CuS NCs surface by reacting the amino moieties of the PEG-coated CuS NCs with *N*-hydroxyl succinic imide-biotin (NHS-biotin), using common EDC-NHS chemistry. The reaction between NHS-biotin and SH-PEG-NH_2-coated NCs can occur spontaneously. However,

DOI: 10.1021/jacs.5b07973
J. Am. Chem. Soc. 2015, 137, 15145−15151

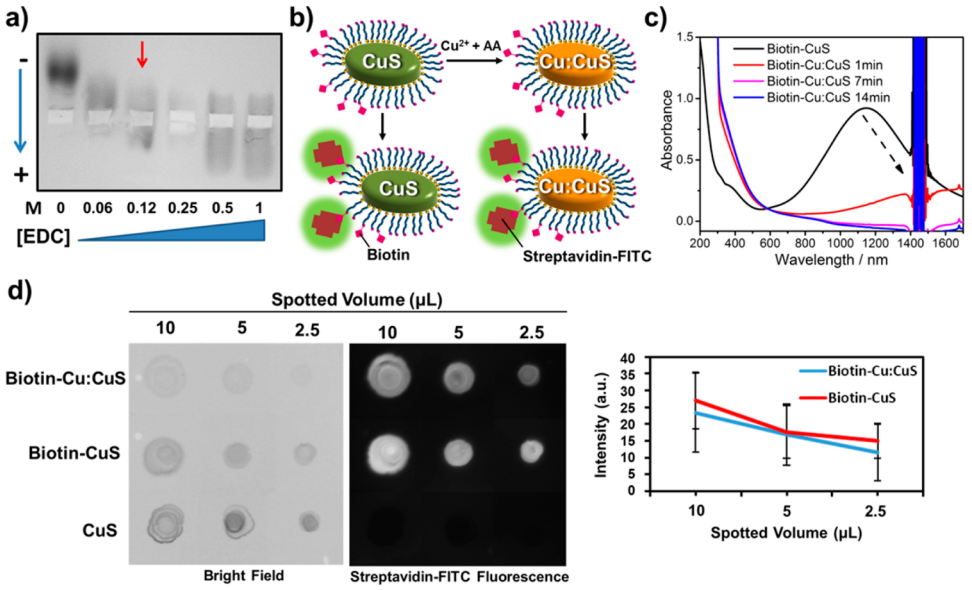

Figure 3. (a) Electrophoretic assay on agarose gel at pH 4.4 (2.5% agarose gel in β-alanine/acetic acid buffer for 1 h at 100 V) of CuS-PEG-NH_2+NHS-biotin mixture with increasing amount of EDC; red arrow indicates the reaction condition chosen for the copper incorporation and streptavidin binding assay. (b) Scheme of incorporation reaction on biotin-CuS with Cu^{2+} in the presence of ascorbic acid and of the binding assay with streptavidin-FITC conjugation on biotin-CuS and biotin-Cu:CuS. (c) Absorption spectra of biotin-CuS upon addition of 1 equiv of Cu^{2+} in the presence of ascorbic acid. (d) Detection of the biotin functionality on the CuS covellite before and after copper incorporation by dot blot assay with streptavidin-FITC and the corresponding quantitative densitometry.

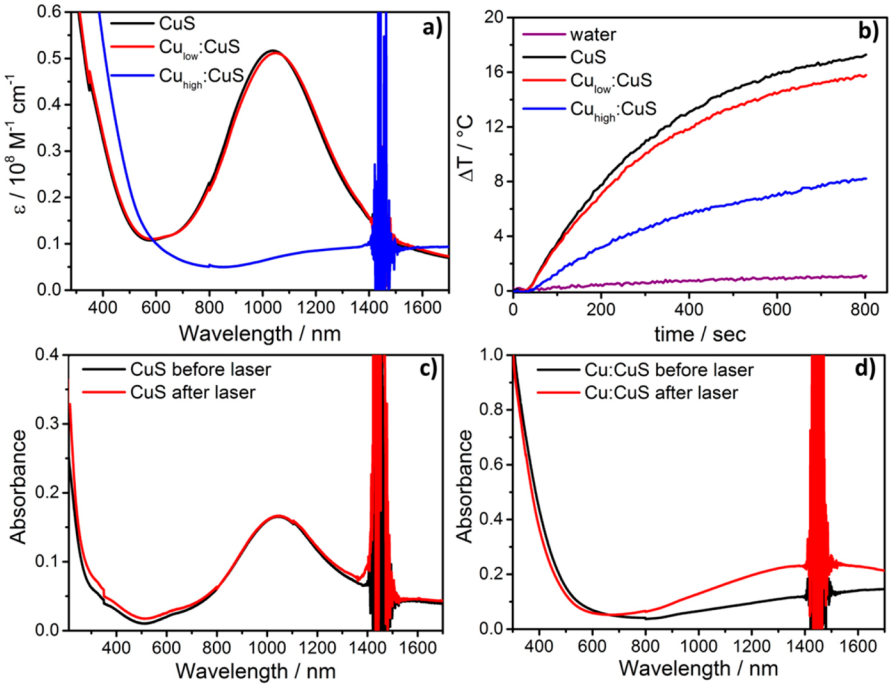

Figure 4. (a) Extinction spectra of CuS NCs (black line), Cu_{low}:CuS NCs (red line), and Cu_{high}:CuS NCs (blue line) in water. (b) Temperature profile of water solution of CuS NCs (5 nM NCs, black curve), Cu_{low}:CuS NCs (5 nM NCs, red curve), and Cu_{high}:CuS NCs (20 nM NCs, blue curve) placed in a quartz cuvette of 1 cm path length under continuous NIR laser irradiation (808 nm, 0.85 W, spot area = 0.49 cm^2) with respect to the same profile recorded on plain water (purple curve). In all cases, the volume of the NCs dispersion or water was 1 mL. (c) Absorption spectra of PEG-CuS water solution before (black curve) and after (red curve) laser irradiation. (d) Absorption spectra of PEG-Cu_{high}:CuS water solution before (black curve) and after (red curve) laser irradiation. In both cases, the spectra were recorded using a 3 mm path length cuvette.

upon increasing the EDC content, the number of biotin molecules associated with each NC could be finely tuned, as shown by the change in the migration behavior of the NCs on gel electrophoresis (Figure 3a). As additional indication of anchoring of the biotin molecules, the overall zeta potential changed from +21 mV, for the plain PEG-CuS NCs (amino terminated), to −4 mV, for the biotin-PEG CuS NCs. We then performed the copper incorporation on these biotin-functionalized CuS NCs (fixed at 0.8 mM of Cu) with 1 equiv of Cu(I) solution. We intentionally followed here a protocol that

DOI: 10.1021/jacs.5b07973
J. Am. Chem. Soc. 2015, 137, 15145−15151

employs a large fraction of Cu ions, in order to observe an appreciable shift on the plasmon peak that validates the successful incorporation. We observed that, when using 1 equiv of Cu(II) and 6 equiv of AA, the incorporation rate was comparable to that of the plain PEG-CuS NCs and was again accompanied by a complete quenching of the NIR plasmon band, compatible with the formation of copper rich biotin-Cu:CuS NCs (Figure 3c). Elemental analysis proved that the amount of copper incorporated in biotin-PEG-CuS NCs was similar to the one incorporated in PEG-CuS NCs. The Cu enrichment was found to be 40% and 49% for PEG-CuS and biotin-PEG-CuS, respectively (Figure S9a), proving that the surface functionality did not significantly impair the incorporation reaction. Also, TEM images of biotin-PEG-CuS NCs and biotin-PEG-Cu:CuS showed no substantial morphological changes of the NCs upon Cu incorporation (Figure S9b).

To evaluate if the Cu incorporation interferes with the biotin binding at the NC's surface toward streptavidin, a dot blot assay was performed (Figure 3d). To this end, fluorescein-streptavidin was added to biotin-CuS or biotin-Cu:CuS NCs spotted on nitrocellulose paper at different NC volume. Similar fluorescence signals from these spots were recorded for Cu:CuS NCs and CuS NCs, underlining minor differences in the binding of streptavidin to CuS or to Cu:CuS NCs. Moreover, no significant differences in densitometry analyses of the resulting fluorescent complexes of CuS-PEG-biotin-streptavidin-FITC and Cu:CuS-PEG-biotin-streptavidin-FITC were observed (Figure 3d). The plain PEG-CuS NCs that underwent the same purification steps were also tested as control, to assess unspecific streptavidin binding. As expected, no fluorescent signal was detected in this case. These results stand as a clear evidence that copper incorporation does not affect the functionality of biotin molecules located at the outer ligand shell. Since this incorporation experiment was done using a much higher amount of Cu precursor than in the radiolabeling experiments described previously, we can conclude that the radiolabeling process with ^{64}Cu does not alter the biotin functionality.

Copper sulfide NCs have a strong localized surface plasmon resonance in the near-infrared region that can be exploited in photothermal therapy for the conversion of adsorbed NIR light into heat.[22,24−30] We show here that our CuS and Cu:CuS NCs exhibit photothermal conversion efficiencies that are comparable with values reported in the literature. First, we compared the molar extinction coefficients at 808 nm (ε_{808}) for CuS NCs, Cu_{low}:CuS NCs (after Cu incorporation and under conditions that are comparable to those followed for the radiolabeling experiment, ^{64}Cu:CuS, meaning 0.0002 equiv Cu(II) with respect to [Cu_{NC}]) and for Cu_{high}:CuS NCs (1 equiv of Cu(II) with respect to [Cu_{NC}]). We noticed that CuS and Cu_{low}:CuS share basically the same ε_{808}, while for Cu_{high}:CuS it is significantly reduced (Figure 4a). If we compare the ε_{808} values for CuS, Cu_{low}:CuS, and Cu_{high}:CuS NCs to other nanomaterials, we notice that in all cases their extinction coefficients are orders of magnitude higher than those of strong absorbing organic dyes, like cyanines, for example,[31,32] and they are at the upper limit compared to other plasmonic particles.[24,25]

Based on these observations, we can state that the photothermal conversion efficiencies of CuS and Cu_{low}:CuS NCs should be practically identical, while differences between CuS NCs or Cu_{low}:CuS NCs and Cu_{high}:CuS NCs are expected. Therefore, we studied the temperature change of an aqueous dispersion of CuS NCs and Cu_{high}:CuS NCs having approximately the same optical density (ca. 0.2) at the irradiation wavelength of 808 nm (Figure 4b). As expected from the high molar extinction coefficients at 808 nm for CuS NCs ($\varepsilon_{808} = 2.3 \times 10^7$ M^{-1} cm^{-1}) and for Cu_{high}:CuS NCs ($\varepsilon_{808} = 5.3 \times 10^6$ M^{-1} cm^{-1}), a remarkable temperature increase of up to 18 °C was observed for the CuS NCs (at only 5 nM) and up to 8 °C for Cu_{high}:CuS NCs (20 nM). Pure water, irradiated under the same conditions, showed only a slight temperature increase of 2.2 °C. Laser irradiation did not affect the colloidal stability neither of the CuS nor of the Cu:CuS NCs samples, although for the Cu_{high}:CuS NCs a weak plasmon band was visible after irradiation, suggesting a partial reoxidation of the NCs (Figure 4d). Instead, the absorption spectra recorded before and after laser treatment of the CuS NCs were practically superimposed (Figure 4c). Following a reported procedure,[33] we could quantify the photothermal efficiency of CuS and Cu_{high}:CuS NCs from heating−cooling cycles to be 53% and 33%, respectively (see Figures S10 and S11, SI for detailed procedure). The values of photothermal conversion efficiencies found for our CuS NCs (and hence also Cu_{low}:CuS NCs) and Cu_{high}:CuS NCs are significantly higher than the ones reported for other copper chalcogenide NCs like Cu_9S_5 (25.7%)[25] and $Cu_{2-x}S$ (16.7%)[30] and just slightly lower than those of the CuS NCs reported by Zou et al. (56.7%).[29] Recently reported polypyrrole-coated chainlike gold NC assemblies (70%)[34] and polymeric nanoparticles based on polyethylenedioxythiophene (71.1%)[35] have evidenced higher photothermal conversion efficiencies. However, most of these particles are much larger in size than those studied here and their absorption cross sections are significantly higher than those of our CuS-based NCs; hence, a direct comparison with our data is not straightforward.

CONCLUSIONS

In summary, the here reported protocol allows to radiolabel covellite CuS NCs with ^{64}Cu(I) ions as a last step in the NC preparation line (e.g., NC synthesis, water transfer and targeting) by simply mixing the NCs in buffer with an aqueous solution of $^{64}CuCl_2$ and vitamin C, at room temperature. The reaction is completed after few minutes, and a simple purification procedure using a desalting column ensures radiolabeling and purification within a time span of around 20 min. The Cu(I) incorporation reaction was found to take place with a comparable efficiency on water-soluble biotin conjugated CuS NCs and on PEGylated CuS NCs, without impairment of the binding functionality of the biotin toward the streptavidin. This fast and effective protocol enables in-house radioactivation/labeling of NCs in, for example, hospitals. This is of utter importance since the routine work of clinical personnel must not be altered with respect to that of classical radiolabeling protocols. Also, the quick protocol (only 20 min for labeling and purification) helps to reduce the exposure of the operator to ionizing radiations, and, at the same time, it shortens the time lag between the ^{64}Cu production and the availability of ^{64}Cu radiolabeled NCs. Also, as shown here, when incorporating a small amount of copper, like in the radiotracer scenario, the covellite Cu_{low}:CuS NCs remain excellent candidates for photothermal ablation. In perspective, we do expect that the ^{64}Cu(I) reaction here set could be easily extended to a list of other chalcogenide NCs.[36,37] In contrast to most other strategies, our radiolabeling protocol fulfills all requirements for complete automation. Moreover, given the photothermal efficiency of CuS NCs, which is unaltered for

DOI: 10.1021/jacs.5b07973
J. Am. Chem. Soc. 2015, 137, 15145−15151

Cu_{low}:CuS NCs with respect to that of CuS NCs, and still remarkable for Cu_{high}:CuS NCs, we propose Cu:CuS NCs as a promising theranostic nanomaterial for both PET imaging and photothermal ablation therapy.

■ ASSOCIATED CONTENT

Supporting Information

The Supporting Information is available free of charge on the ACS Publications website at DOI: 10.1021/jacs.5b07973.

Detailed synthesis, water transfer and materials and methods section, Cu(I) and ^{64}Cu(I) incorporation reaction, stability tests of ^{64}Cu-CuS NCs, TGA and XRD characterizations, biotin-NCs conjugation reaction, biotin−streptavidin Dot-blot assay, photothermal set up and heat efficiency calculation are reported (PDF)

■ AUTHOR INFORMATION

Corresponding Author

*teresa.pellegrino@iit.it

Author Contributions

⊥A.R., T.A., and A.C. have contributed equally to this work.

Notes

The authors declare no competing financial interest.

■ ACKNOWLEDGMENTS

The authors are grateful for financial support from the Italian AIRC project (Contract No. 14527 to T.P.), from the Cariplo foundation (Contract No. 2013 0865 to T.P.), and from the Italian FIRB projects (Nanostructured oxides, Contract No. 588 BAP115AYN).

■ REFERENCES

(1) Lewis, J. S.; Laforest, R.; Buettner, T. L.; Song, S. K.; Fujibayashi, Y.; Connett, J. M.; Welch, M. J. *Proc. Natl. Acad. Sci. U. S. A.* **2001**, *98*, 1206−1211.

(2) Shokeen, M.; Anderson, C. J. *Acc. Chem. Res.* **2009**, *42*, 832−841.

(3) Cutler, C. S.; Hennkens, H. M.; Sisay, N.; Huclier-Markai, S.; Jurisson, S. S. *Chem. Rev.* **2013**, *113*, 858−883.

(4) Hong, H.; Zhang, Y.; Sun, J.; Cai, W. *Nano Today* **2009**, *4*, 399−413.

(5) Jarrett, B. R.; Gustafsson, B.; Kukis, D. L.; Louie, A. Y. *Bioconjugate Chem.* **2008**, *19*, 1496−1504.

(6) Pombo-Garcia, K.; Zarschler, K.; Barreto, J. A.; Hesse, J.; Spiccia, L.; Graham, B.; Stephan, H. *RSC Adv.* **2013**, *3*, 22443−22454.

(7) Xie, J.; Chen, K.; Huang, J.; Lee, S.; Wang, J. H.; Gao, J.; Li, X. G.; Chen, X. Y. *Biomaterials* **2010**, *31*, 3016−3022.

(8) Xie, J.; Liu, G.; Eden, H. S.; Ai, H.; Chen, X. Y. *Acc. Chem. Res.* **2011**, *44*, 883−892.

(9) Cai, W. B.; Chen, K.; Li, Z. B.; Gambhir, S. S.; Chen, X. Y. *J. Nucl. Med.* **2007**, *48*, 1862−1870.

(10) Schipper, M. L.; Cheng, Z.; Lee, S. W.; Bentolila, L. A.; Iyer, G.; Rao, J. H.; Chen, X. Y.; Wul, A. M.; Weiss, S.; Gambhirl, S. S. *J. Nucl. Med.* **2007**, *48*, 1511−1518.

(11) Schipper, M. L.; Iyer, G.; Koh, A. L.; Cheng, Z.; Ebenstein, Y.; Aharoni, A.; Keren, S.; Bentolila, L. A.; Li, J. Q.; Rao, J. H.; Chen, X. Y.; Banin, U.; Wu, A. M.; Sinclair, R.; Weiss, S.; Gambhir, S. S. *Small* **2009**, *5*, 126−134.

(12) Bass, L. A.; Wang, M.; Welch, M. J.; Anderson, C. J. *Bioconjugate Chem.* **2000**, *11*, 527−532.

(13) Boswell, C. A.; Sun, X. K.; Niu, W. J.; Weisman, G. R.; Wong, E. H.; Rheingold, A. L.; Anderson, C. J. *J. Med. Chem.* **2004**, *47*, 1465−1474.

(14) Kreyling, W. G.; Abdelmonem, A. M.; Ali, Z.; Alves, F.; Geiser, M.; Haberl, N.; Hartmann, R.; Hirn, S.; de Aberasturi, D. J.; Kantner, K.; Khadem-Saba, G.; Montenegro, J. M.; Rejman, J.; Rojo, T.; de Larramendi, I. R.; Ufartes, R.; Wenk, A.; Parak, W. J. *Nat. Nanotechnol.* **2015**, *10*, 619−623.

(15) Yang, S. Y.; Sun, S. S.; Zhou, C.; Hao, G. Y.; Liu, J. B.; Ramezani, S.; Yu, M. X.; Sun, X. K.; Zheng, J. *Bioconjugate Chem.* **2015**, *26*, 511−519.

(16) Zhao, Y. F.; Sultan, D.; Detering, L.; Cho, S. H.; Sun, G. R.; Pierce, R.; Wooley, K. L.; Liu, Y. J. *Angew. Chem., Int. Ed.* **2014**, *53*, 156−159.

(17) Zhou, M.; Zhang, R.; Huang, M. A.; Lu, W.; Song, S. L.; Melancon, M. P.; Tian, M.; Liang, D.; Li, C. *J. Am. Chem. Soc.* **2010**, *132*, 15351−15358.

(18) Sun, X. L.; Huang, X. L.; Guo, J. X.; Zhu, W. L.; Ding, Y.; Niu, G.; Wang, A.; Kiesewetter, D. O.; Wang, Z. L.; Sun, S. H.; Chen, X. Y. *J. Am. Chem. Soc.* **2014**, *136*, 1706−1709.

(19) Liang, W.; Whangbo, M. H. *Solid State Commun.* **1993**, *85*, 405−408.

(20) Melancon, M. P.; Zhou, M.; Li, C. *Acc. Chem. Res.* **2011**, *44*, 947−956.

(21) Xie, Y.; Riedinger, A.; Prato, M.; Casu, A.; Genovese, A.; Guardia, P.; Sottini, S.; Sangregorio, C.; Miszta, K.; Ghosh, S.; Pellegrino, T.; Manna, L. *J. Am. Chem. Soc.* **2013**, *135*, 17630−17637.

(22) Goel, S.; Chen, F.; Cai, W. B. *Small* **2014**, *10*, 631−645.

(23) *CRC Handbook of Chemistry and Physics*, 92nd ed.; Haynes, W. M., Ed.; CRC Press: Boca Raton, FL, 2011; p 196.

(24) Hessel, C. M.; Pattani, V. P.; Rasch, M.; Panthani, M. G.; Koo, B.; Tunnell, J. W.; Korgel, B. A. *Nano Lett.* **2011**, *11*, 2560−2566.

(25) Tian, Q. W.; Jiang, F. R.; Zou, R. J.; Liu, Q.; Chen, Z. G.; Zhu, M. F.; Yang, S. P.; Wang, J. L.; Wang, J. H.; Hu, J. Q. *ACS Nano* **2011**, *5*, 9761−9771.

(26) Hsu, S. W.; On, K.; Tao, A. R. *J. Am. Chem. Soc.* **2011**, *133*, 19072−19075.

(27) Zhao, Y. X.; Burda, C. *Energy Environ. Sci.* **2012**, *5*, 5564−5576.

(28) Li, W. H.; Zamani, R.; Rivera Gil, P.; Pelaz, B.; Ibanez, M.; Cadavid, D.; Shavel, A.; Alvarez-Puebla, R. A.; Parak, W. J.; Arbiol, J.; Cabot, A. *J. Am. Chem. Soc.* **2013**, *135*, 7098−7101.

(29) Li, B.; Wang, Q.; Zou, R. J.; Liu, X. J.; Xu, K. B.; Li, W. Y.; Hu, J. Q. *Nanoscale* **2014**, *6*, 3274−3282.

(30) Wang, S. H.; Riedinger, A.; Li, H. B.; Fu, C. H.; Liu, H. Y.; Li, L. L.; Liu, T. L.; Tan, L. F.; Barthel, M. J.; Pugliese, G.; De Donato, F.; Scotto D'Abbusco, M.; Meng, X. W.; Manna, L.; Meng, H.; Pellegrino, T. *ACS Nano* **2015**, *9*, 1788−1800.

(31) Mujumdar, R. B.; Ernst, L. A.; Mujumdar, S. R.; Lewis, C. J.; Waggoner, A. S. *Bioconjugate Chem.* **1993**, *4*, 105−111.

(32) Camerin, M.; Jori, G.; Della Ciana, L.; Fabbroni, S.; Bonacchi, S.; Montalti, M.; Prodi, L. *Photochem. Photobiol. Sci.* **2009**, *8*, 1422−1431.

(33) Roper, D. K.; Ahn, W.; Hoepfner, M. *J. Phys. Chem. C* **2007**, *111*, 3636−3641.

(34) Lin, M.; Guo, C.; Li, J.; Zhou, D.; Liu, K.; Zhang, X.; Xu, T.; Zhang, H.; Wang, L.; Yang, B. *ACS Appl. Mater. Interfaces* **2014**, *6*, 5860−5868.

(35) Li, L.; Liu, Y.; Hao, P.; Wang, Z.; Fu, L.; Ma, Z.; Zhou, J. *Biomaterials* **2015**, *41*, 132−140.

(36) Li, H. B.; Brescia, R.; Krahne, R.; Bertoni, G.; Alcocer, M. J. P.; D'Andrea, C.; Scotognella, F.; Tassone, F.; Zanella, M.; De Giorgi, M.; Manna, L. *ACS Nano* **2012**, *6*, 1637−1647.

(37) Comin, A.; Manna, L. *Chem. Soc. Rev.* **2014**, *43*, 3957−3975.

DOI: 10.1021/jacs.5b07973
J. Am. Chem. Soc. 2015, 137, 15145−15151